[3]Alkabie, H. S., Andrews, G. E., and Ahmed, H. T., "Lean Low NO_x Primary Zones Using Radial Swirlers," American Society of Mechanical Engineers, New York, ASME Paper 88-GT-245, June 1988.

[4]Quagliaroli, T. M., Laufer, G., Krauss, R. H., and McDaniel, J. C., Jr., "Laser Selection Criteria for OH Fluorescence Measurements in Supersonic Combustion Test Facilities," *AIAA Journal*, Vol. 31, No. 3, 1993, pp. 520–527.

[5]Seitzman, J. M., Palmer, J. L., Antonio, A. L., Hanson, R. K., DeBarber, P. A., and Hess, C. F., "Instantaneous Planar Thermometry of Shock-Heated Flows Using PLIF of OH," AIAA Paper 93-0802, Jan. 1993.

[6]Battles, B. E., Seitzman, J. M., and Hanson, R. K., "Quantitative Planar Laser-Induced Fluorescence Imaging of Radical Species in High Pressure Flames," AIAA Paper 94-0229, Jan. 1994.

Single-Pulse Temperature Measurement in Turbulent Flame Using Laser-Induced O_2 Fluorescence

J. H. Grinstead*
Princeton University, Princeton, New Jersey 08544
and
T. M. Quagliaroli,† G. Laufer,‡ and J. C. McDaniel Jr.§
University of Virginia, Charlottesville, Virginia 22903

Introduction

TEMPORALLY resolved measurements of flowfield variables, such as temperature, density, velocity, and species concentration, are important for the study of turbulent reacting and nonreacting flows. Such measurements can provide data on probability distributions that are unattainable with time-averaged techniques. Short-duration impulse facilities such as shock tubes, shock tunnels, or combustion bombs that are employed in high-speed aerodynamic and combustion research require instrumentation with precise timing as well as high time resolution. As temperature is an important parameter in these studies, several time-resolved laser-spectroscopic thermometry techniques have been developed and demonstrated. Unfortunately, only a few techniques are sufficiently versatile for widespread use. In general, these techniques are tailored to specific measurement requirements, exploit certain thermodynamic conditions or constraints in the gas flow under study, and/or are applied to problems for which their strengths are particularly suited.

A new single-pulse, two-line laser-induced O_2 fluorescence temperature measurement technique has recently been developed[1] for use in unseeded high-temperature (1500–3000 K) reacting and nonreacting airflows where temperature, pressure, and species concentrations are subject to turbulent fluctuation. The technique has been characterized and calibrated in a high-temperature atmospheric air furnace. Here, we demonstrate its potential for use in high-temperature reacting flows with measurements in the turbulent postflame gases of a premixed, atmospheric propane–O_2 flame.

Presented as Paper 95-0423 at the AIAA 33rd Aerospace Sciences Meeting, Reno, NV, Jan. 10–13, 1995; received Feb. 15, 1995; revision received June 30, 1995; accepted for publication Oct. 30, 1995.

*Postdoctoral Research Associate, Department of Mechanical and Aerospace Engineering, Engineering Quadrangle, Room D414, Olden Street.

†Graduate Research Assistant, Aerospace Research Laboratory, 570 Edgemont Road. Student Member AIAA.

‡Associate Professor, Aerospace Research Laboratory, 570 Edgemont Road. Senior Member AIAA.

§Professor, Aerospace Research Laboratory, 570 Edgemont Road. Member AIAA.

Temperature Measurement Technique

The technique is based on the simultaneous excitation of the spectrally coincident $v'(0) \leftarrow v''(6)P(13)$ and $v'(2) \leftarrow v''(7)R(11)$ absorption lines in the $B^3\Sigma_u^- - X^3\Sigma_g^-$ Schumann–Runge system of O_2 using a tunable KrF laser. The peaks of these lines near 40,251 cm^{-1} (248.44 nm) overlap each other within ~0.05 cm^{-1}. Because of their close proximity, a single laser with a bandwidth of approximately 1 cm^{-1} can excite both lines simultaneously. As a result, the fluorescence from both upper states reached by absorption is emitted simultaneously as well. Although separation of the two fluorescence contributions by time-resolved detection is not possible, unique features of their emission spectra allow them to be separated spectroscopically. By using a spectrometer equipped with a multichannel array detector, the fluorescence spectrum resulting from the excitation of both lines can be recorded on a single-pulse basis. Thus, by analyzing each single-pulse dispersion spectrum, time-resolved thermometry is realized. Although limited to point or line measurements, this approach is simpler than alternative two-line laser-induced fluorescence (LIF) approaches,[2,3] where two lasers and two detection systems are needed for time-resolved thermometry. Unlike single-pulse Rayleigh or Raman techniques, which require high laser pulse energies (~200 mJ) to produce a sufficiently high single-pulse signal-to-noise ratio, this LIF technique requires only 5–10 mJ and thereby precludes problems associated with particle incandescence as well as with exceeding damage thresholds of window materials. Owing to the high predissociation rate of the upper states, quenching corrections are unnecessary for pressure up to approximately 2 atm—an important consideration in turbulent reacting flows where the local gas composition is subject to considerable fluctuation. However, the low fluorescence conversion efficiency and restrictions on the incident laser flux present with this O_2 LIF technique[1] may limit its use to high-temperature flows with greater than trace concentrations of O_2. Although LIF detection limits are intimately tied to particular experimental configurations, the detection limit realized in the present experiment was estimated to be ~0.5% mole fraction at 2500 K and 1 atm.

The technique was calibrated in a high-temperature atmospheric air furnace where independent thermocouple measurements were available.[1] Mean temperatures and their variances were obtained from 100 single-pulse measurements at furnace temperatures from 1300 to 1800 K, and the mean temperatures were compared with the corresponding thermocouple measurements. For 100-pulse averages, typical measurement error over this range was 1.3%. Photon shot noise was found to be the primary source of error in the fluorescence measurements. The measured standard deviation in the single-pulse LIF temperature measurements in the furnace agreed well with the predicted uncertainty computed using the mean temperature and fluorescence signals. Single-pulse temperature measurement uncertainties (1σ) in atmospheric air ranged from approximately 13% at 1300 K to 7% at 1800 K. The theoretical model[1] that was used to accurately interpret the temperature dependence of the fluorescence signals measured in the furnace was also used in the present demonstration to determine temperatures outside the calibration range. Since the coefficients that were determined from the calibration measurements are temperature independent, such extrapolation outside of the calibration range is justified. In addition, systematic errors in the temperature measurement due to uncertainties in the model parameters were found to be small relative to propagated uncertainties in the single-pulse fluorescence signal measurement.[4]

Turbulent Flame Temperature Measurements

To demonstrate the technique's viability for measurements in reacting gas flows where the O_2 concentration and temperature are subject to turbulent fluctuation, temperature measurements were obtained in the turbulent high-temperature gases of a premixed propane–O_2 jet flame. The flame was produced by a commercially available, atmospheric pressure blast burner commonly used for glass and metal shaping. The intense, axisymmetric turbulent flame was approximately 15 mm in length and was located approximately 5 mm above the burner tip (D = 1 mm). The luminous region of the postflame gases extended approximately 150 mm above the base of

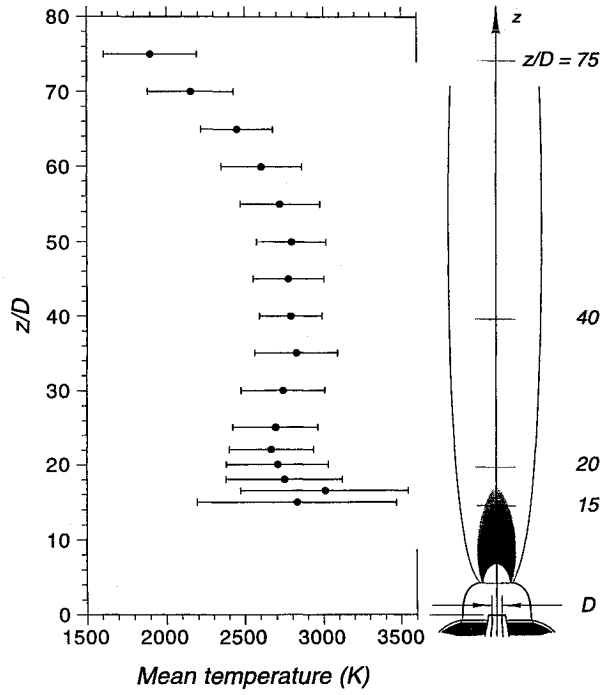

Fig. 1 Variation of mean temperatures in an atmospheric propane–O_2 flame with normalized distance z/D along the centerline axis of burner. The error bars represent 1σ limits of 100 single-pulse measurements. The diagram to the right shows the nominal flame location relative to the measurement points.

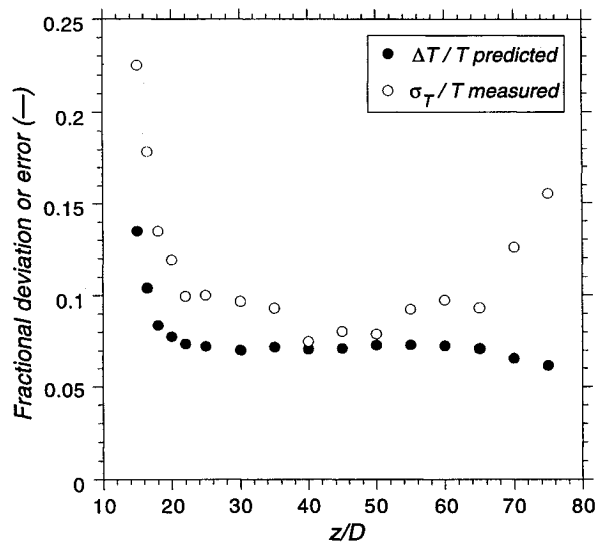

Fig. 2 Filled circles represent the variation of the predicted single-pulse measurement uncertainty $\Delta T/T$ with nondimensional distance z/D corresponding to the measurements of Fig. 1, and the open circles show the variation of measured fractional standard deviation σ_T/T with distance corresponding to the measurements of Fig. 1.

the flame. The burner was run as a free jet in atmospheric air with no coflow. Measurements were made near the tip of the flame region and in the postflame gases.

The experimental apparatus is similar to that outlined in Ref. 1. The KrF laser beam directed to the flame was unfocused and spatially apertured to a 1.5 × 1.5 mm^2 cross section. The segment of the beam coinciding with the centerline of the burner axis was imaged onto the 1-mm-wide entrance slit of a 0.5 mf/6.9 spectrometer. A two-lens telescope with f/3.5 collection imaged the fluorescence from the flame with 2:1 magnification; the dimensions of the measurement volume were thus 1.5 × 1.5 × 0.5 mm^3. An intensified charge-coupled device array placed at the exit plane of the spectrometer was used as the detector. Since the predissociated O_2 fluorescence occurs only during the laser pulse, the realized time resolution was approximately 20 ns. Prior and subsequent to obtaining fluorescence spectra in the flame, fluorescence spectra in a high-temperature atmospheric air furnace were obtained for calibration purposes.

Figure 1 shows the variation of temperature with nondimensional distance z/D above the burner exit plane along the centerline axis. Each point represents a mean of 100 single-pulse measurements, and the error bars correspond to one standard deviation (σ_T) of the 100 measurements. Adjacent to the plot of Fig. 1 is a diagram showing the approximate flame structure relative to the measurement points. The lowest point ($z/D = 15$) is located nominally within the visible tip of the flame. At points closer to the burner exit, where the O_2 concentration falls below the detection limit, the fluorescence signals were too weak for a reliable temperature measurements. The remainder of the points reside in the postflame region. The mean temperatures are seen to range from approximately 3000 K at $z/D = 16.5$ to approximately 1900 K at $z/D = 75$.

Because of the turbulent nature of the flow, the variance in each of these temperature measurements represents a combination of two components: the variance due to the measurement uncertainty and that due to turbulence-induced temperature fluctuations. Although the individual contributions of each of these components cannot be separated experimentally, the effect of measurement uncertainty can be estimated. Previous experiments[1] have demonstrated that for fluorescence signal levels comparable to that of the present experiment, the temperature measurement uncertainty $\Delta T/T$ is controlled primarily by the photon shot noise. Therefore, the actual uncertainty $\Delta T/T$ can be accurately estimated from the magnitude of the fluorescence signal and the inferred temperature. Figure 2 shows the variation of the estimated $\Delta T/T$ of each of the mean temperatures with distance z/D. At low z/D, where the O_2 concentration is low, the single-pulse uncertainty in the fluorescence signal and, subsequently, the temperature measurement are high. Farther away from the flame, air entrainment within the postflame gases increases the magnitude of the fluorescence signal and lowers the temperature measurement uncertainty. For comparison, the measured fractional standard deviation σ_T/T of the corresponding 100 single-pulse temperatures at each z/D location is also shown. Although not negligible, the measurement uncertainty $\Delta T/T$ is consistently smaller than σ_T/T, thereby indicating that the error bars of Fig. 1 are extended by the turbulence-induced fluctuations. In effect, the distribution obtained from a series of measurements represents the convolution of a measurement error distribution function (due primarily to photon shot noise in the fluorescence measurements) and an actual turbulence-induced temperature distribution. With the exception of three points (z/D = 40, 45, and 50), where the magnitude of the turbulent fluctuations is comparable to $\Delta T/T$, an estimate of the turbulent fluctuations can be discerned by comparing the measured fluctuations and the predicted measurement uncertainty. Although not attempted here, net turbulent temperature distributions can be recovered from measured distributions by using appropriate measurement error distribution functions, obtained either from measurements in a quiescent environment or by assuming normally distributed, shot-noise-limited fluorescence measurements.

Conclusions

Time-resolved pointwise temperature measurements in the high-temperature gases of a turbulent, premixed propane–O_2 atmospheric pressure flame were demonstrated using a new single-pulse KrF laser-induced O_2 fluorescence temperature measurement technique. The technique is based on simultaneous excitation of two spectrally coincident transitions followed by spectrally resolved multichannel fluorescence detection. The accuracy of the fluorescence signal measurements was limited by photon shot noise and was therefore controlled by the magnitude of the fluorescence signals. In a quiescent environment, the accuracy of temperature measurements is limited by this fluorescence measurement uncertainty. However, in the turbulent flame employed for these measurements, the effect of turbulent fluctuations in most regions of the postflame gas was shown to exceed the single-pulse measurement uncertainty. The combined rms deviation of turbulence-induced temperature fluctuations and measurement uncertainty, σ_T/T, varied from 8 to 23%,

whereas the estimated contribution due to measurement uncertainty varied from 6 to 13%. Therefore, these measurements can also be used to estimate the extent of the turbulent fluctuations. In addition, since each temperature measurement is obtained from simultaneous measurements of fluorescence signals from two independent transitions, linear averaging of a series of temperature measurements is permissible; the possible systematic error in the temperature derived from averaged, nonsimultaneous fluorescence measurements is avoided with this technique. With a relatively high data rate (~5 Hz), a well-characterized measurement uncertainty, and the ability to be extended to line imaging, this new instantaneous temperature measurement technique can provide single-pulse measurements in high-temperature reacting flows where temperature, pressure, and species concentrations are subject to turbulence-induced fluctuations.

References

[1]Grinstead, J. H., Laufer, G., and McDaniel, J. C., Jr., "Single-Pulse, Two-Line Temperature Measurement Technique Using KrF Laser-Induced O_2 Fluorescence," *Applied Optics*, Vol. 34, No. 24, 1995, pp. 5501–5512.

[2]Seitzman, J. M., Hanson, R. K., DeBarber, P. A., and Hess, C. F., "Application of Quantitative Two-Line OH Planar Laser-Induced Fluorescence for Temporally Resolved Planar Thermometry in Reacting Flows," *Applied Optics*, Vol. 33, No. 18, 1994, pp. 4000–4012.

[3]McMillin, B. K., Palmer, J. L., and Hanson, R. K., "Temporally Resolved, Two-Line Fluorescence Imaging of NO Temperature in a Transverse Jet in Supersonic Cross Flow," *Applied Optics*, Vol. 32, No. 36, 1993, pp. 7532–7545.

[4]Grinstead, J. H., "Temperature Measurement in High-Temperature Gases Using KrF Laser-Induced O_2 Fluorescence," Ph.D. Dissertation, Dept. of Mechanical, Aerospace, and Nuclear Engineering, Univ. of Virginia, Charlottesville, VA, Jan. 1995.

Multiple-Time-Scale Turbulence Model Computations of Flow over a Square Rib

E. Zeidan* and N. Djilali†
University of Victoria,
Victoria, British Columbia V8W 3P6, Canada

Introduction

TURBULENT flow separation is commonly encountered in both internal and external flows with abrupt changes in geometry. Practical examples of such flows are found in heat exchangers, turbomachinery, combustors, heating and ventilation systems, and cooling of electronic components. The flow over a surface mounted obstacle or rib considered here is related to the classical backward-facing-step geometry but is somewhat more complex because of the formation of multiple primary and secondary recirculation zones and their interaction. The rib geometry provides a good laboratory configuration for further understanding of the physics of flow separation and for evaluating turbulence models and numerical discretization procedures.[1]

The classical two-equation k–ε eddy viscosity model (EVM) and its variants have been the most widely used engineering models to compute separated flows. The performance of these models in separated flows is unsatisfactory in many respects,[2,3] even with the substantial improvements brought about by corrections to account for extra strain effects an streamline curvature.[3,4] One of the weaknesses of EVMs is the use of a single time (or length) scale to characterize the turbulence. This leads to poor predictions of the eddy viscosity in flow situations where large departures from equilibrium conditions occur.

One approach to address this problem is multiscale (MS) turbulence modeling, first proposed by Hanjalić et al.,[5] which consists of partitioning the energy spectrum into several regions, each characterized by a different time scale. In the simplified split-spectrum method used by Kim and Chen,[6] turbulent transport is described by using two time scales: the first corresponds to the large energy-bearing eddies and describes generation of turbulent kinetic energy, and the second corresponds to the smaller-scale eddies and describes dissipation rate. In this Note we examine the performance of Kim and Chen's MS model in high Reynolds number flow over two-dimensional surface-mounted ribs. The computations are performed using a finite volume method with a higher order quadratic upwind scheme, which is stable and conservative and which incorporates an upstream-weighted curvature correction.

Turbulence Model

To account for the evolution of the different scales in the large-eddy production range and the small-eddy dissipation range, the turbulent energy spectrum can be partitioned into three regions:

1) Production region, characterized by the turbulent kinetic energy k_p and the energy transfer rate ε_p.

2) Transfer region, characterized by the turbulent kinetic energy k_t and the dissipation rate ε_t.

3) Dissipation region, where the turbulent kinetic energy is dissipated into heat.

Kim and Chen's MS turbulence model formulation[6] used in this study is based on a single-point closure with a variable spectrum-partitioning method. The location of the partition, or the ratio k_p/k_t, is determined as part of the solution and is dependent on the turbulence intensity, production, transfer, and dissipation rates. The partition is moved toward the high-wave number region when production is high and towards the low-wave number region when production is low. Turbulent transport is described by using a time scale characterizing large eddies, and the dissipation rate is characterized by using the fine-scale eddies.

The turbulent kinetic energy and the energy transfer rate equations for the energy containing large eddies are given by[6]

$$\frac{\partial(\rho U_i k_p)}{\partial x_i} - \frac{\partial}{\partial x_i}\left\{\left(\mu + \frac{\mu_t}{\sigma_{k_p}}\right)\frac{\partial k_p}{\partial x_i}\right\} = \rho G_k - \rho\varepsilon_p \tag{1}$$

$$\frac{\partial(\rho U_i \varepsilon_p)}{\partial x_i} - \frac{\partial}{\partial x_i}\left\{\left(\mu + \frac{\mu_t}{\sigma_{\varepsilon_p}}\right)\frac{\partial \varepsilon_p}{\partial x_i}\right\} = C_{p1}\frac{\rho G_k^2}{k_p} + C_{p2}\frac{\rho G_k \varepsilon_p}{k_p} - C_{p3}\frac{\rho \varepsilon_p^2}{k_p} \tag{2}$$

The turbulent kinetic energy and dissipation rate equations for the fine-scale eddies are given by

$$\frac{\partial(\rho U_i k_t)}{\partial x_i} - \frac{\partial}{\partial x_i}\left\{\left(\mu + \frac{\mu_t}{\sigma_{k_t}}\right)\frac{\partial k_t}{\partial x_i}\right\} = \rho\varepsilon_p - \rho\varepsilon_t \tag{3}$$

$$\frac{\partial(\rho U_i \varepsilon_t)}{\partial x_i} - \frac{\partial}{\partial x_i}\left\{\left(\mu + \frac{\mu_t}{\sigma_{\varepsilon_t}}\right)\frac{\partial \varepsilon_t}{\partial x_i}\right\} = C_{t1}\frac{\rho \varepsilon_p^2}{k_t} + C_{t2}\frac{\rho\varepsilon_p\varepsilon_t}{k_t} - C_{t3}\frac{\rho\varepsilon_t^2}{k_t} \tag{4}$$

where the production rate is given as

$$G_k = \frac{\mu_t}{\rho}\left\{2\left(\frac{\partial U}{\partial x}\right)^2 + 2\left(\frac{\partial V}{\partial y}\right)^2 + \left(\frac{\partial U}{\partial y} + \frac{\partial V}{\partial x}\right)^2\right\}$$

and the empirical coefficients are determined by examining limiting cases of asymptotic turbulence growth and decay rates and

Received April 5, 1995; revision received Oct. 17, 1995; accepted for publication Oct. 18, 1995.

*Graduate Research Assistant, Department of Mechanical Engineering.

†Associate Professor, Department of Mechanical Engineering. Member AIAA.